MANTECH Publications

Journal of Electrical Power System Engineering and Technology
Volume 7, Issue 3, September-December, 2022

Verification of Rotor & Grid Side Converter (RSC & GSC) Model of DFIG Wind Turbine

Suryaprasad Yamana[1], Chetan Danam[2]
Assistant Professor[1], Student[2]
Department Electrical Engineering
MLR Institute of Technology
Corresponding Author's Email: - *damanchetan225@gmail.com[2]*

Abstract

The PI regulator is coupled with terms in the current's d&q components to control the current in a closed loop. All of these second-order transfer functions can be used to accurately model all of the current loops based on reference transformations (such as DQ-ABC and Phase Locked Loop). By using the second order system, the current control model will be compared to the equivalent closed loop current control transfer function. This method makes calculating the PI regulator control gain simple. When comparing the output of the current control loop with its equivalent current control transfer function, use the unitary step response. The inverse-Laplace transform will then be applied, with the natural frequency dictating the dynamic behaviour into the exponential term.

Keywords: *Second order transfer function, Current control Loop, Unitary step response & Inverse Laplace Transform, PI regulator.*

INTRODUCTION

Due to their environmental friendliness, lack of adverse environmental effects, cost effectiveness, and superior efficiency compared to other generators, doubly fed induction generator based wind turbines are now widely used to generate electricity throughout the world. The stator and rotor are the two components of a doubly fed induction generator. The stator is directly connected to the grid, and the rotor is connected to the grid in part via a back-to-back (Power Electronics) converter that has two sides: one on the rotor and one on

the grid. Rotor and grid side converter control is the control method used for both side converters [1, 2 and 3].

The current control loop [4 and 5] is a common feature of the controls for the grid and rotor side converters. In this paper, a closed loop second order transfer function will be used to simplify these current loops. Because it includes a PI regulator in the d and q components of the current with coupling terms and a phase-locked looked loop, among other things, both sides of the converter control inside construction are quite complicated. This complexity can be accurately modelled as a second order transfer function.

The transfer function [6–7] is the ratio of a linear system's output to its input. Only differences in impedance and resistance, such as Lr, Rr, and Lg, Rg for the rotor and grid side converters, respectively, differentiate our model's current control loop from that of both side converters. Here is a representation of the resistance and inductance (R and L) in their general form since both side current control loops are nearly identical [8].

The mathematical term, this current loops general simplified can be found equivalent standard denominator of the second order system, the simplified term of the denominator of the second order system have a damping factor ξ(zita) . In our model has been used critical damping like $\xi = 1$.After that comparing the two second order system closed loop transfer model to get PI Regulator current control gain (Kp& Ki).Then apply the unitary step response for comparing the result between the current control loop & equivalent current control transfer function.

The inverse Laplace transform will then be used to apply the dynamic behaviour, which is provided by the natural frequency, into the exponential term. When applying a unitary step response after using the Laplace transform, the first term generally causes a second dynamic response, depending on how much the first term differs from the second term. This difference indicates the amplitude's size. This overshoot may be greater or less severe.

MATERIALS AND METHODS

B. Second order current control close loop of RSC & GSC

The closed loop RSC behave is simplified way as a second order transfer function with a zero & two poles. The close loop current control consists coupling terms

with PI regulator in d&q component of the current (Fig. 2).

All these current loops (Fig. 1) based on reference transformation (like DQ-abc)soon & Phase locked loop so on, that is quit complex thing can be make accurately model as transfer function of second order.

The RSC current control loops which these parts together with Phase locked loop that can be simplified to represent & quit accurately as this transfer function the d & q current loops are the same.

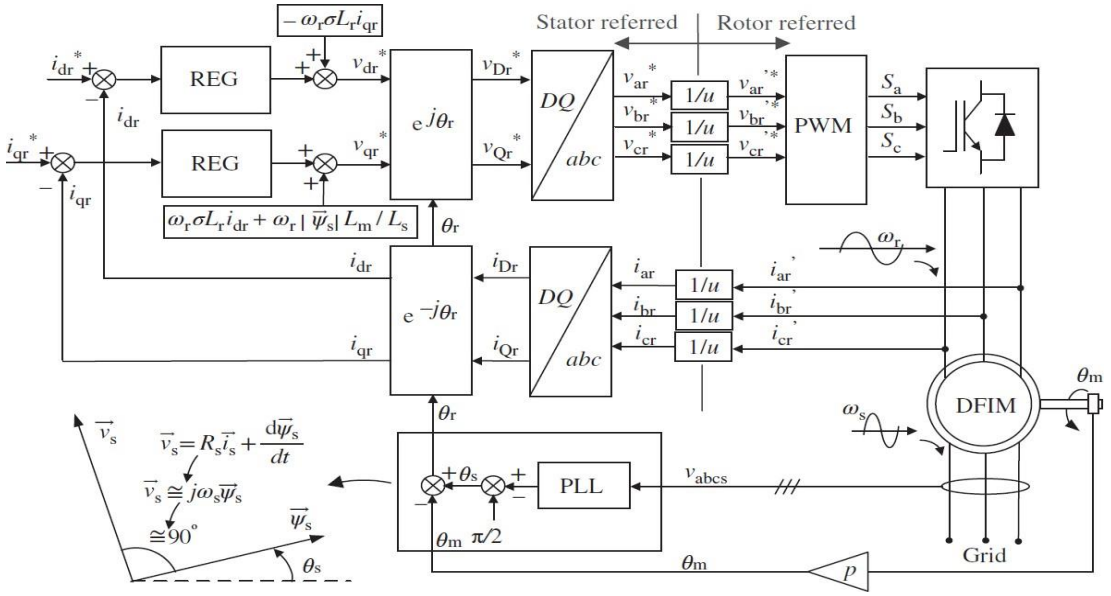

Fig: 1. DFIG Rotor side current control loop

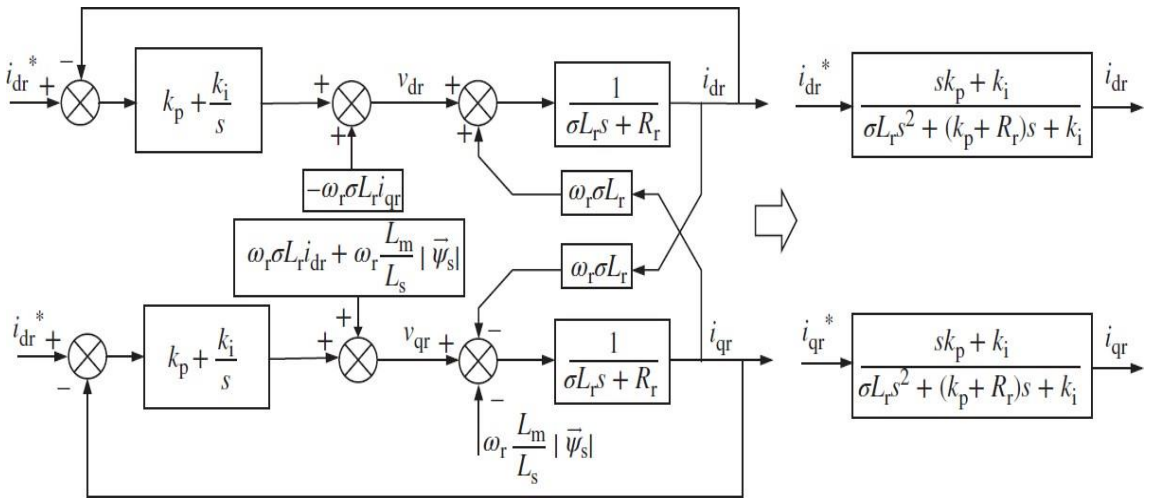

Fig: 2. Equivalent closed Current control loop include PI regulators of RSC

In the same away, in GSC current loops can be simplified d & q current loops to transfer function of 2nd order system with a zero & two poles (Fig. 3)

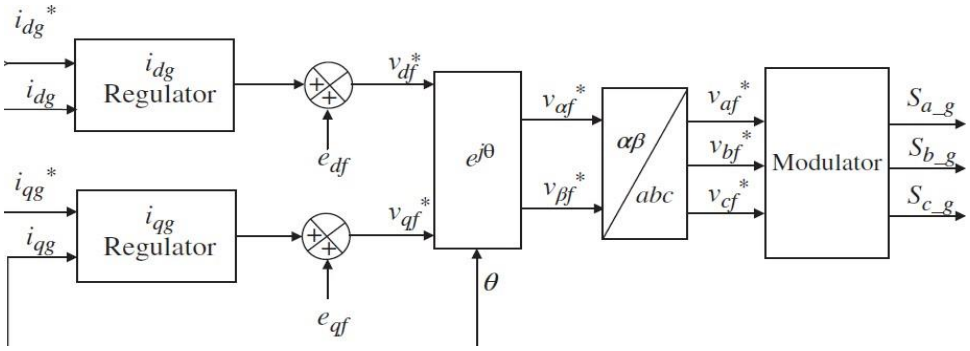

Fig: 3 Grid Side Converter Current Control loop of DFIG

For analyzing the closed current control loops in more generic away need to realize the behavior of transfer function of Rotor & grid side converter. Now here will show the general form of the current control closed loops second order close loop system after that illustrate the details current control loops of RSC & GSC.

$$\frac{i_{ds}(s)}{i_{qs}(s)} = \frac{i_{dr}(s)}{i_{qr}(s)} = \frac{\frac{(k_p s+k_i)}{L}}{s^2+\left(\frac{k_p+R}{L}\right)S+\frac{k_i}{L}} \quad \ldots\ldots\ldots (1)$$

Where, L & R are the general inductance & resistance of RSC & GSC.

This is current loops general simplified of can found equivalent standard denominator of the second order system.

$$\begin{cases} \frac{i(s)}{i^*(s)} = \frac{\frac{(k_p s+k_i)}{L}}{s^2+2\xi\omega_n s+\omega_n^2} \\ \quad = \frac{\frac{(k_p s+k_i)}{L}}{(s+\omega_n)^2} \end{cases} \ldots\ldots\ldots\ldots (2) \qquad [\xi = 1]$$

Where, Damping factor/ratio, (zita), ωn = Natural frequency

So, we get kp & ki value from equations (1) & (2)

$$k_p = 2\omega_n L - R \& k_i = \omega_n^2 L \ \ldots\ldots\ldots (3)$$

Where, k_p& K_i is the control gain of the Proportion & integral (PI) regulator

Unitary Unit response

$$i(s) = \frac{\frac{(k_p s + k_i)}{L}}{s(s+\omega_n)^2}$$

$$i(s) = \frac{\frac{k_p}{L}}{(s+\omega_n)^2} + \frac{\frac{k_i}{L}}{s(s+\omega_n)^2} \quad \ldots\ldots\ldots\ldots (4)$$

Now applying the inverse Laplace in equation (4)

$$i(t) = \frac{k_p}{L} t e^{-\omega_n t} + \frac{k_i}{L\omega_n^2}(1 - e^{-\omega_n t} - \omega_n e^{-\omega_n t}) \quad \ldots\ldots\ldots (5)$$

& achieve the temporal current in function of time

$$i(t) = \frac{1}{L}\left(k_p - \frac{k_i}{\omega_n}\right) t e^{-\omega_n t} + \frac{k_i}{L\omega_n^2}(1 - e^{-\omega_n t}) \quad \ldots\ldots\ldots\ldots (6)$$

Steady state condition, $e^{-\omega n t} = 0$ so,

$$i(t) = \frac{k_i}{L\omega_n^2} = \frac{\omega_n^2 L}{L\omega_n^2} = 1. \quad [k_i = \omega_n^2 L]$$

Where dynamic behavior is given by ωn in these exponential term $(e^{-\omega_n t})$. In General, this term $\left(k_p - \frac{k_i}{\omega_n}\right) t e^{-\omega_n t}$ is responsible for the another shoot at the dynamic response when apply ωn unitary step response & depending how much is the difference between 1st term $\left(k_p - \frac{k_i}{\omega_n}\right)$ of ωn equation (5). This difference means how big the amplitude. This overshoot $(e^{-\omega_n t})$) could be bigger or smaller.

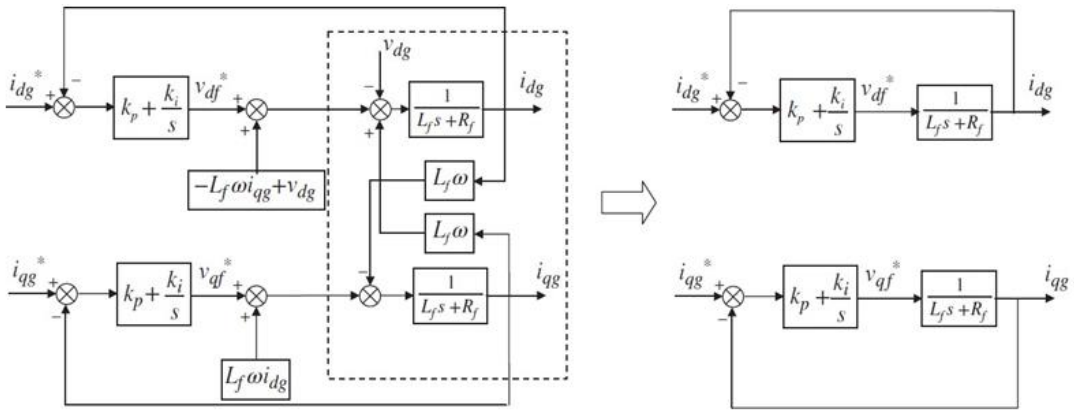

Fig: 4 Equivalent closed Current control loop include PI regulators of GSC

C. Step Response & Bode Diagram (RSC & GSC)

When amplitude is more than 1 that term is called overshoot. For RSC, at time 0.02s it reaches steady state condition but for GSC it reaches steady state at time 0.015s. Basically it is real pole dynamic system.

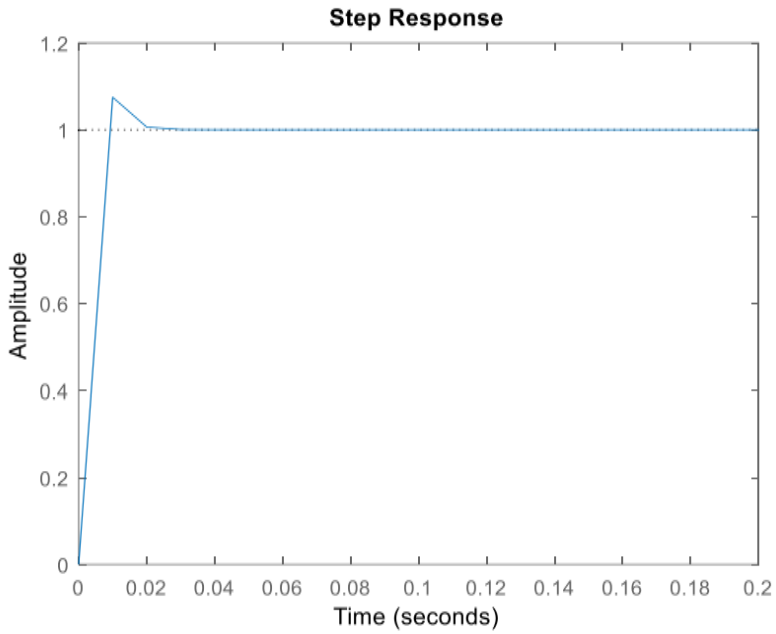

(a)

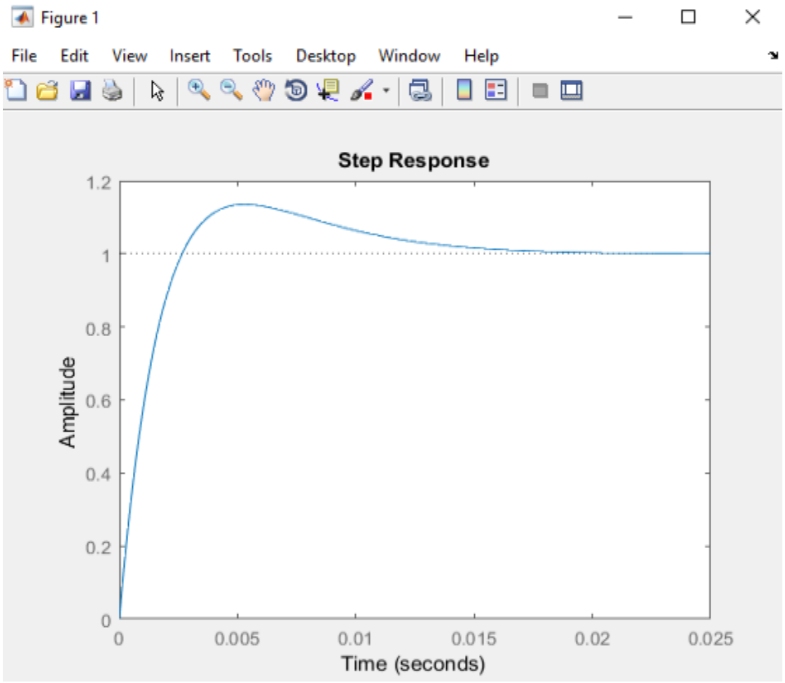

(b)

Fig: 5. Step response of Rotor & grid side converter control (a, b)

Bode Diagram:

This is the close loop behavior of the current loop grid & rotor side converter with the band width very similar.

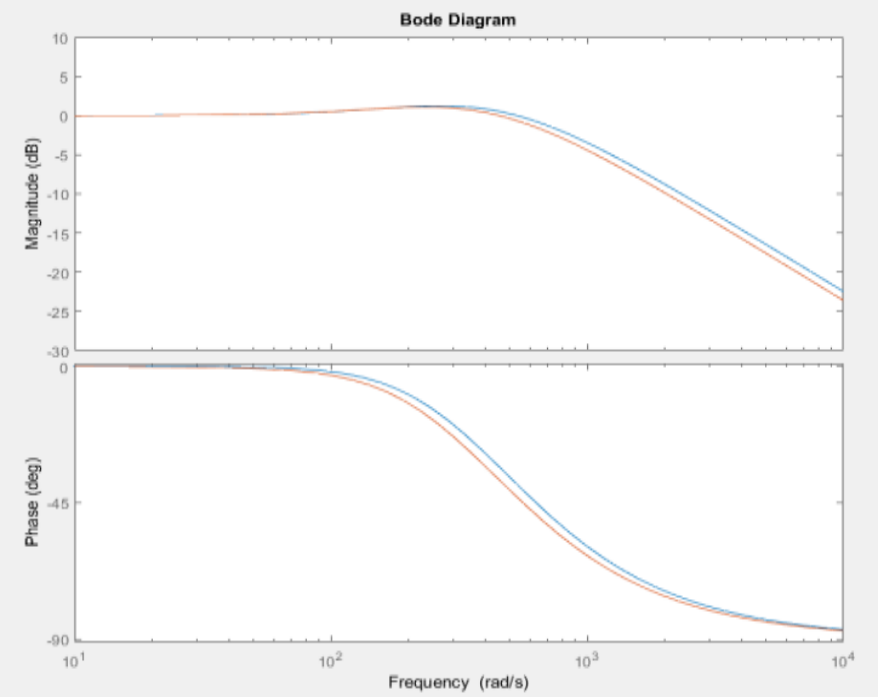

Fig: 6. Bode diagram of Rode & grid side converter at blue & orange lines respectively

D. Understanding the current regulator error for the digital delay

In Fig. 7 the black line is the voltage references (Sinusoidal reference voltage), they are changing over the time. Here have sampling that measurement of the current then algorithm needs some times to do calculation & once finish the calculation then PWM output is perform just one sample period later in the next triangular. This is one delay that is considered between the RSC / GSC controller & PWM based on the sampled current with 1.5 sampling interval like 1.5Tsw.

During the sampling interval of the synchronous rotating reference frame is simultaneously to the outputs of PI regulator current. Current will be sampled at the beginning time‘t’& the algorithm of regulator is accomplished from the beginning time‘t’. 1st sampling period‘t’ convert to t + Tsw. Then the up-to-date Signals of PWM are operated for subsequent sampling period like t + Tsw to t + 2Tsw. During the algorithm the rotating synchronous reference frame rotates ϑ to ϑ+Tswωwhere ωis the constant synchronous speed. The average voltage is:

$$V_{dqs}^{*} = \frac{1}{T_{sw}} \int_{T_{sw}}^{2T_{sw}} V * e^{j(\tau\omega+\vartheta)} d\tau$$

$$V_{dqs}^{*} = k(\omega, T_{sw}) * V * e^{j(1.5\omega T_{sw}+\vartheta)}$$

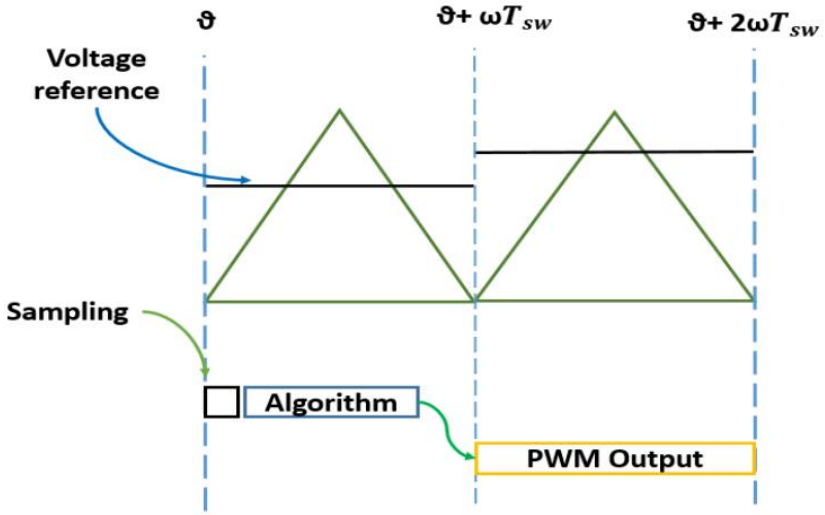

Fig: 7. Sampling Current & PWM Time Outline.

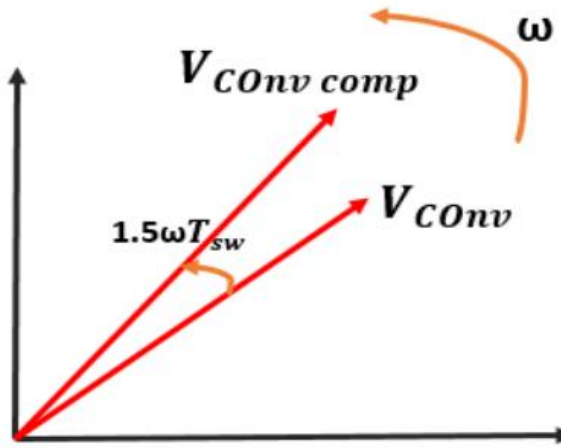

Fig: 8. Synchronous rotor reference frame as time passes

For these terms (ω, Tsw) & $1.5\omega Tsw$ magnitude & phase angle error has been occurred respectively. These errors can be minimized by production of the minimization function.

$$1.5\omega T_{sw} * e^{j(1.5\omega T_{sw})}$$

$$1.5\omega T_{sw} * e^{j(1.5\omega T_{sw})}$$

Sampling frequency, $f_{sw} = \frac{1}{T_{sw}}$, magnitude error is negligible because it is less than 5% whereas, Phase angle error is considered because its angle error is 27 degree at $f = f_{sw}/20$ 1 that is degraded the current regulator performance.

E. Simulation result of current loop (RSC& GSC)

In this case switching frequency 4KHz, this delay hasat the between the control and modulation is not so big, no need to bigger but just in case need to communicate lower switching frequency. It should do it in order to more accurate with the theoretical dynamic response that is predicted so the step has been made and new steady state has been reached.

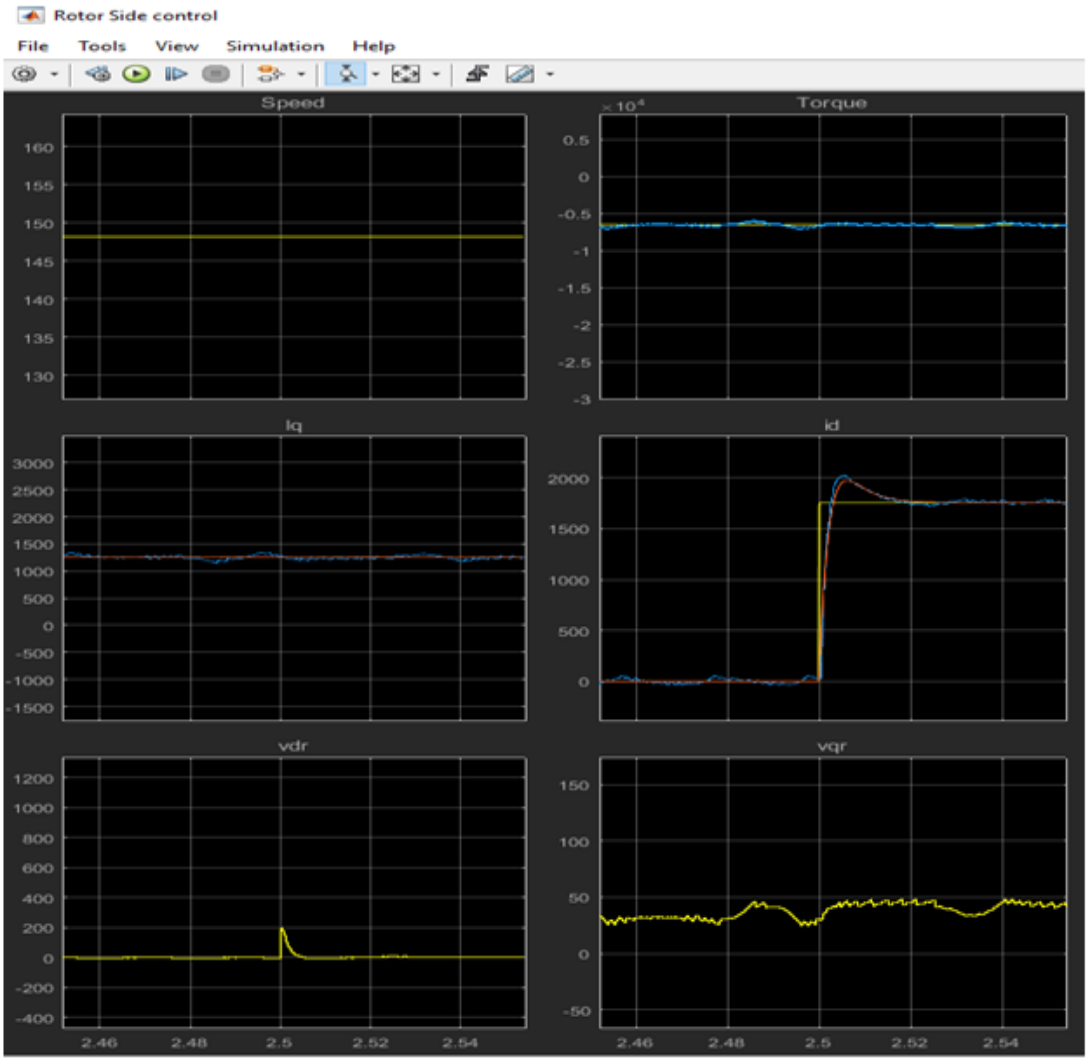

Fig. 9. Simulation result of current control loop validation of Rotor side converter

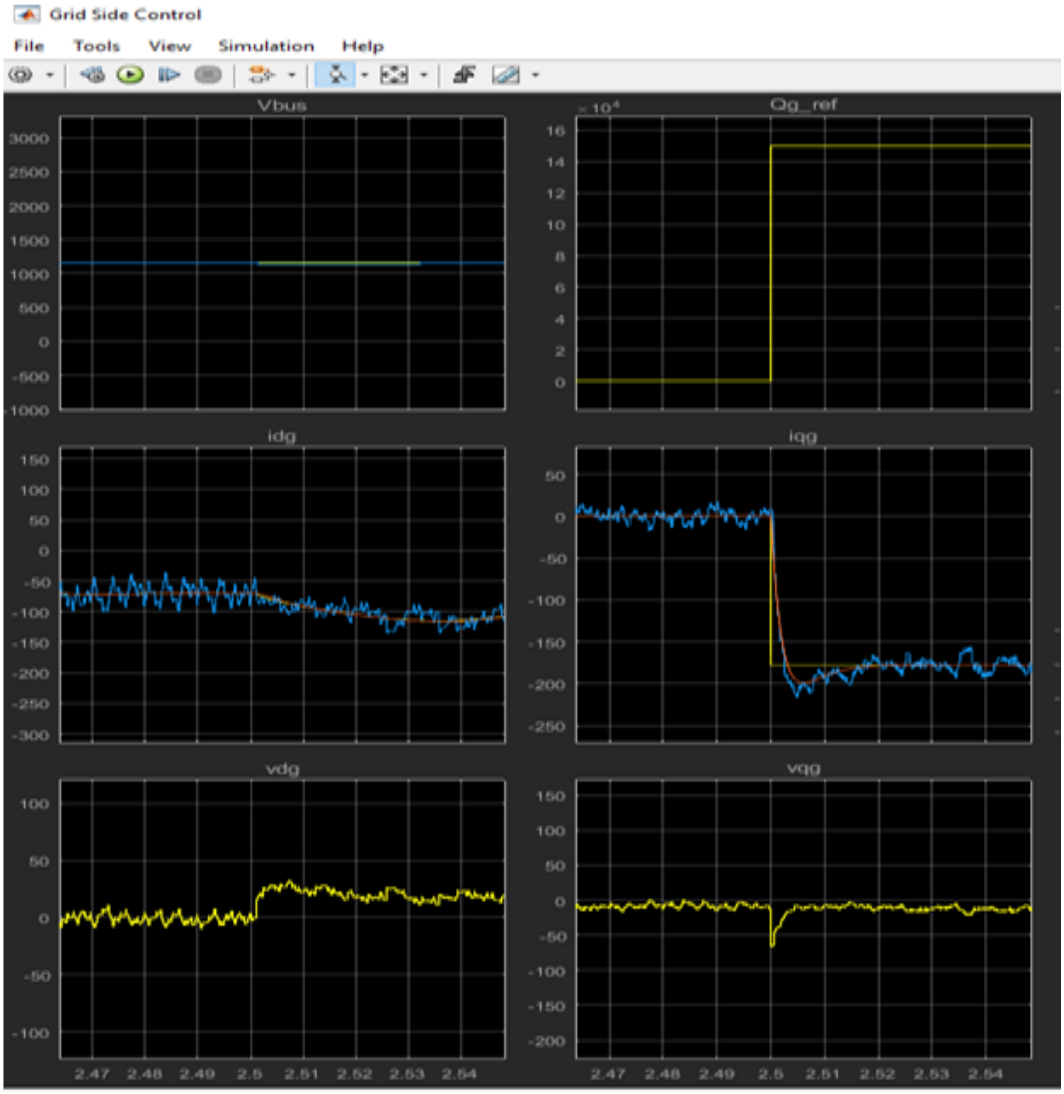

Fig: 10. Simulation result of current control loop validation of Grid side converter

CONCLUSION

By contrasting the current control model with the equivalent closed loop current control of the second order transfer system of the both side converter control, this paper attempts to demonstrate the accuracy of our system model (rotor and grid side converter control). A second order transfer function with a zero and two poles is a simplified representation of how the closed loop RSC behaves. Applying the second order transfer function will enable you to quickly determine the PI current regulator gain. using the compensation to offset the current regulator error for the digital delay. Here, sampling is used to measure the current. Once the algorithm has completed its calculations, the PWM output is performed just one sample period later in the following triangular. The RSC/GSC

controller and PWM take this delay into account based on the sampled current with a 1.5 sampling interval. Finally, by analysing the current control loop using a second order transfer function, a more accurate result was obtained.

REFERENCES

1. Muhammad Sanaullah ;Masud H Chowdhury: 'A new real pole delay model for RLC interconnect using second order approximation', IEEE 57th International Midwest Symposium on Circuits and Systems (MWSCAS), 2014.
2. Haitham Abu-Rub, Mariusz Malinowski, Kamal Al-Haddad, "Book: POWER ELECTRONICS FOR RENEWABLE ENERGY SYSTEMS, TRANSPORTATION AND INDUSTRIAL APPLICATIONS", IEEE Press, 2014 John Wiley & Sons Ltd.
3. GONZALO ABAD (Mondragon University, Spain): 'Power Electronics and Electric Drives for Traction Applications', John Wiley & Sons, Ltd., This edition first published 2017.
4. Doubly fed induction Generator, Wikipedia. (https://en.wikipedia.org/wiki/Doubly- fed_electric_machine)
5. Xueliang Wei, 'Study on Digital PI Control of Current Loop in Active Power Filter', IEEE, INSPEC Accession Number: 11642759, 11 November 2010.
6. E. Goepel,: 'Active RC networks: what benefit is there in having conjugate real zeros in the second-order transfer function?' IEEE International Symposium on Circuits and Systems (IEEE Cat. No.04CH37512), 2004.
7. Shenghu Li, Jiejie Huang &Zhengfeng Wang, 'Inner-loop current control for low-voltage ride- through of permanent-magnet synchronous generator', IECON 2017 - 43rd Annual Conference of the IEEE Industrial Electronics Society.
8. XiyunYang ; Wei Liu ; Peng Wei ; Jinxia Li , 'A new modeling method based on the power — Power transfer function': Year: 2011 , Conference Paper , IEEE.
9. Jing, Xin, "Modeling and Control of a Doubly Fed Induction Generator for Wind Turbine Generator System" (2012). Master's Thesis (2009-). Paper 167.
10. Meera G. S, N. A Divya, 'Rotor side converter of DFIG based wind

energy conversion system', IJERT, ISSN: 2278-0181, Vol. 4 Issue, August-2015.

11. B. Bryant ; M.K. Kazimierczuk, 'Open-loop power-stage transfer functions relevant to current- mode control of boost PWM converter operating in CCM', IEEE Transactions on Circuits and Systems I: Regular Papers, Volume: 52, Issue: 10 , Journal Article , IEEE, 2005.
12. Ren Jingding ;CheYanbo ; Chen Xi,: 'Research on rotor-side converter based on DSP for double fed wind power generation system', 4th International Conference on Power Electronics Systems and Applications, Conference Paper | Publisher: IEEE, Year: 2011.

    T. Samina ; S. Rama Iyer ; A. BisharathuBeevi,: 'Rotor side control for improving the transient response of Doubly fed induction generator in wind power system'; International Conference on Technological Advancements in Power and Energy (TAP Energy), Conference Paper , Publisher: IEEE, 2017.
13. Zhao yang Su; Ping Wang ; Pengxian Song,: 'Research on control strategy of DFIG rotor side converter', Conference Paper, IEEE, 2014.
14. Sushanta Kumar Senapati ; Ashish Kumar Swain,: 'Modeling and simulation of AC/DC grid side voltage source converter used in wind power generation system', International Conference on Circuits, Power and Computing Technologies [ICCPCT-2014], IEEE, 2014.
15. Haiyan Tang ; Wei He ; Yongning Chi ; Xinshou Tian ; Yan Li ; Yukun Wang,: 'Impact of grid side converter of DFIG on sub-synchronous oscillation and its damping control'; IEEE PES Asia-Pacific Power and Energy Engineering Conference (APPEEC); 2016.
16. Shunsu ke Yamaki ; Masahide Abe ; Masayuki Kawamata,: 'Transfer functions of second- order digital filters with two equal second-order models' , IEEE International Symposium on Circuits and Systems (ISCAS), 2012.
17. KaikaiWang ; Yao Wang ; Zhe Cheng ; Lihua Liu ; LinliJia ; Yan Liang,: 'Research on Reactive Power Control of the Grid-Side Converter of DFIG Based Wind

Farm', 2nd IEEE Conference on Energy Internet and Energy System Integration (EI2), IEEE, Conference Paper,2018.

18. GuofengYuan ;Ruipeng Liang: 'A DFIG wind turbine low-voltage ride-through control strategy based on resynchronization of rotor side converter', 2017 China International Electrical and Energy Conference (CIEEC), Conference Paper , Publisher: IEEE , Conference Paper , Publisher: IEEE, Year: 2017 .